

Noise-controlled pattern formation and threshold shift for electroconvection in the conduction and dielectric regimes

Jong-Hoon Huh,¹ Akiyuki Kuribayashi,¹ and Shoichi Kai²

¹*Department of Mechanical Information Science and Technology, Faculty of Computer Science and Systems Engineering, Kyushu Institute of Technology, Fukuoka 820-8502, Japan*

²*Department of Applied Quantum Physics and Nuclear Engineering, Faculty of Engineering, , Kyushu University, Fukuoka 812-8581, Japan*

(Received 10 August 2009; published 7 December 2009)

We report noise-controlled electrohydrodynamic pattern formations and threshold shifts in nematic liquid crystals. In the electrohydrodynamic system superposed with noise, experimental results obtained in the dielectric regime are compared to those in the conventional conduction regime. The noise intensity dependences of thresholds and pattern evolution processes are remarkably different for each regime. The pattern formation mechanisms in the presence of noise for both regimes are discussed based on the results. Moreover, it is found that the thresholds and characteristic wavelengths of dissipative structures can be effectively controlled by external multiplicative noises with appropriate intensity and correlation times.

DOI: [10.1103/PhysRevE.80.066304](https://doi.org/10.1103/PhysRevE.80.066304)

PACS number(s): 47.54.-r, 61.30.Cz, 61.30.Eb

I. INTRODUCTION

Pattern formation in spatially extended dissipative systems driven far from equilibrium is common in nature. Many examples exist in fluid physics, chemistry, biology, and numerous other fields [1]. Owing to the progress of theoretical and numerical studies and experiments, the universal aspects of various patterns in fluid systems are in the process of being understood, at least near the primary instability [1,2]. In this paper, we address ac-driven electrohydrodynamic convections (EHCs) in anisotropic fluids [i.e., nematic liquid crystals (NLCs)] that provide a rich variety of patterns. These have been intensively studied for last four decades [2–8] since they were first observed by Williams [9] and theoretically dealt with by Carr and Helfrich [10,11].

The essential features of EHCs can be easily understood in a planarly aligned NLC system [$\mathbf{n}_0=(1,0,0)$ for the initial director state; see below for details] [2,5,12,13]. When one applies a sinusoidal ac field $\mathbf{E}(t)=E_0 \sin(2\pi ft)\hat{\mathbf{z}}$ across a thin slab between two electrode plates (typical thickness $d=10\text{--}100\ \mu\text{m}$), one observes convective roll patterns beyond a threshold voltage (V_c). For EHCs in such anisotropic fluids, the director \mathbf{n} , a unit vector representing the locally averaged orientation of rodlike molecules of NLCs, plays an important role in pattern formation. Any director fluctuation leads to inhomogeneous charge distribution in the system owing to the electric conduction anisotropy of NLCs ($\Delta\sigma\neq 0$). If the resulting Coulomb force above V_c overcomes the viscous force, material flow is induced. This flow in turn gives rise to a torque on the director, by which the fluctuations of the director are reinforced. Consequently, electrohydrodynamic instability is induced, which leads to EHCs. At low frequencies below a certain characteristic frequency f^* , in general, the charge relaxation time τ_σ is much shorter than the period f^{-1} of $\mathbf{E}(t)$ ($\tau_\sigma f\ll 1$), while the director relaxation time τ_d is much larger than f^{-1} ($\tau_d f\gg 1$). Therefore, in the so-called *conduction* regime, the director cannot follow the external field $\mathbf{E}(t)$ and remains stationary to leading order. In the (high-frequency) *dielectric* regime ($f>f^*$), on the other hand, τ_σ becomes larger than f^{-1} ($\tau_\sigma f\gg 1$), and charges can-

not accumulate. The director oscillates in phase with the ac field $\mathbf{E}(t)$, while the charge distribution is stationary.

In general, EHCs are considered in the abovementioned two regimes. The typical patterns are widely known as Williams domains (WDs) and chevron patterns (CVs) (herringbone-like patterns) in the corresponding regimes [5,12,13], as shown in Fig. 1. Here, we deal with the CVs found in the dielectric regime although other types of CVs such as defect-mediated CVs and defect-free CVs are often observed in the conduction regime [14]. Their thresholds and characteristic wavelengths (λ_{WD} for WDs and λ_1 and λ_2 for CVs, shown in Fig. 1) can be easily varied by controlling external fields and the conditions of NLC samples (e.g., material constants and thickness d). In this paper, we report the variation in the thresholds and wavelengths of these WDs and CVs observed in *external multiplicative noise* processes. It is well known that noises play an important role in bifurcation phenomena in nonlinear dissipative systems. For instance, stochastic resonance [15,16], noise-induced order and disorder [17–20], and multiplicative stochastic processes [21–24] are well-known nontrivial effects of noise. A noise-induced shift in thresholds for instabilities has been reported for many different systems [17,18]. In particular, the present ac-driven electrohydrodynamic system has been intensively studied from this point of view [21,22,25–34].

Previously reported results for the effects of noise on EHCs are as follows: (i) the superposition of multiplicative noise (with intensity V_N) gives rise to a shift in the deterministic threshold voltage (V_c) for WDs [21,22,25–32]. For relatively small-intensity noise, the threshold satisfies the linear relation $V_c^2=V_{c0}^2+bV_N^2$, where V_{c0} indicates the threshold voltage in the absence of noise ($V_N=0$). That is, the stabilization effect of noise is obtained (i.e., $b>0$). The slope b of the linear relation is a function of the correlation time (τ_N) of the noise [28,29,33]. At certain correlation times τ_N comparable to the characteristic time of the system ($\tau_0\sim 1/2\pi f^*$), the slope becomes flat (i.e., no effect of the stochastic noise is induced; $b=0$). For $\tau_N>\tau_0$, the slope becomes negative ($b<0$). That is, the destabilization effect of the noise can be realized. (ii) A direct transition to turbulence and an ex-

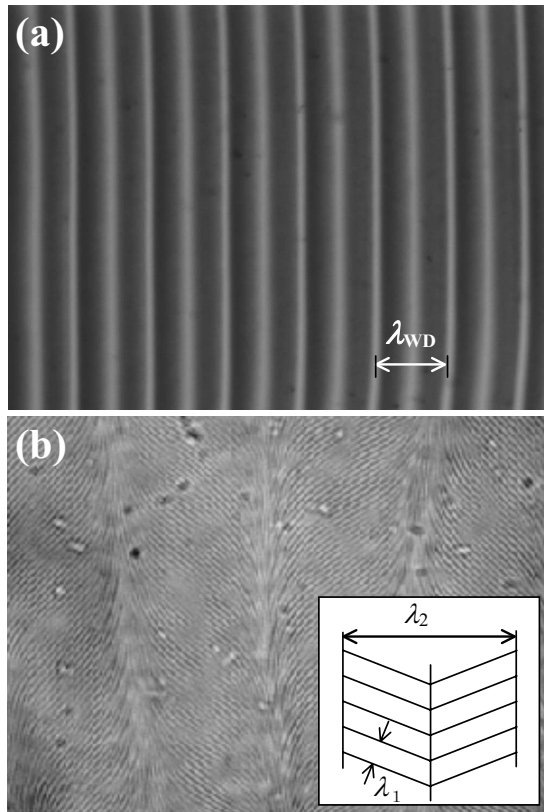


FIG. 1. Typical patterns induced by electrohydrodynamic instability in nematic liquid crystals. (a) Williams domain (WD) in the (low-frequency) conduction regime ($f < f^*$). (b) Chevron pattern (CV) in the (high-frequency) dielectric regime ($f > f^*$). The patterns are characterized by wavelengths λ_{WD} for WDs and λ_1 and λ_2 for CVs, respectively.

change of stable structures were observed for larger V_N [26,28]. (iii) The nonlinear onset time for the appearance of the patterns was measured as a function of V_N [26,28,29]. (iv) Recently, the wave-number dependence of the threshold V_c and noise-dominated patterns for the primary instability were reported [32]. (v) The difference in the noise-induced threshold shift between planarly and homeotropically aligned cells has been reported [34]. (vi) Pure noise-induced EHCs were also investigated. On-off intermittency of EHCs was found in dichotomous noises [31], and stable EHCs in Gaussian noises [34] sufficiently colored ($\tau_N \gg \tau_0$) even in the absence of deterministic ac field. (vii) In theoretical studies, on the other hand, the observed linear relation was successfully explained although the physical approaches used were quite different [21,22,25,27,29–31]. (viii) Behn *et al.* successfully reproduced the wave-number dependence of noise in their stochastic stability model [30]. Thus far however, in past experimental and theoretical studies, many aspects of stochastic effects on instability problems and pattern formations in nonlinear dissipative systems remains unclear.

In this paper, our aim is to present the stochastic effects on EHCs in the dielectric regime as well as the conventional conduction regime and to compare the experimental results for both regimes. Unfortunately, no investigation of these effects has been carried out in the dielectric regime because

these are more difficult to treat theoretically and experimentally than those in the conduction regime. In particular, the variation in characteristic thresholds and wavelengths for both regimes is investigated in τ_N (or cutoff-frequency f_c)-dependent noises superposed on the ac voltage. Moreover, we show pattern evolutions that contain a variety of patterns [WDs, CVs, wormlike patterns (WP), and turbulent patterns] with increasing noise intensity V_N or ac voltage V .

This paper is organized as follows. The details of the present sample cell and the experimental apparatus and techniques are described in Sec. II. In Sec. III A, we present typical thresholds and wavelengths in the absence of noise. In Sec. III B, the effects of noise on the ac thresholds for EHCs are investigated in the conduction and dielectric regimes. The mechanisms for noise-induced pattern formations are discussed for both regimes. In Sec. III C, noise-controlled wavelengths and pattern evolutions are described for both regimes. These are investigated using white or colored noise. Deterministic voltage-controlled pattern evolutions in the dielectric regime are described in Sec. III D in order to compare these to stochastic noise-controlled pattern evolutions. In Sec. IV, our experimental results regarding the effects of noise on EHCs are summarized, and the prospects for future study and application are mentioned.

II. EXPERIMENT

A sinusoidal ac field $E(t)$ superposed with an external multiplicative noise $N(t)$ was applied across a thin slab of an NLC [*p*-methoxybenzylidene-*p'*-*n*-butylaniline (MBBA)] sandwiched between two parallel transparent electrodes (indium tin oxide). A Gaussian-type noise $N(t)$ created by a wave-generating synthesizer (Hioki 7075) and amplified by a wide-range amplifier ($0 < f \leq 500$ kHz, FLC Electronics A600) was used. In particular, cutoff-frequency (f_c)-dependent colored noise was generated from the low-pass filters of the synthesizer, which allows low-frequency signals to pass through but attenuates signals with frequencies higher than f_c . The cut-off frequency f_c of noise is generally defined as a certain frequency value at which the power output becomes half the passband power ($f < f_c$). In this paper, the stochastic intensity $V_N = \sqrt{\langle N^2(t) \rangle} d$ and f_c (inversely proportional to the correlation time τ_N) of the noise $N(t)$ and the deterministic intensity $V = \sqrt{\langle E^2(t) \rangle} d$ and frequency f of the ac field $E(t)$ were used as control parameters. The thickness d of the nematic slab between transparent electrode surfaces given planarly aligning treatment [$\mathbf{n}_0 = (1, 0, 0)$] was $50 \mu\text{m}$, and the lateral (active) size was $1 \times 1 \text{ cm}^2$. The patterns were observed in the xy plane parallel to the electrodes using a charge-coupled-device camera (Sony XC-75) mounted on a polarizing microscope (Meijitech ML9300). To capture and analyze the patterns on a computer, image-processing software (Scion Image Beta 4.0.2) and an image capture board (PCI-VE5, Scion Corporation) were used. All measurements were carried out at a stable temperature ($T = 25 \pm 0.2 \text{ }^\circ\text{C}$) using an electrothermal control system (TH-99, Japan Hightech). At this temperature, the electric conductivities and dielectric constants of the NLC in our sample cell were $\sigma_{\parallel} = 8.99 \times 10^{-8} \Omega^{-1} \text{ m}^{-1}$, σ_{\perp}

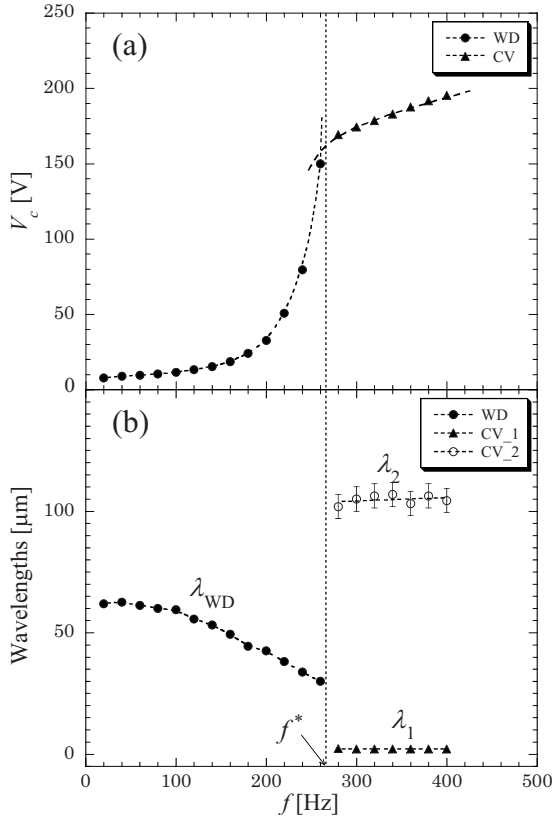


FIG. 2. In the absence of noise: (a) ac frequency dependence of thresholds V_c and (b) wavelengths λ_{WD} for WDs and λ_1 and λ_2 for CVs. Here, f^* (~ 265 Hz) is a characteristic frequency dividing the conduction ($f < f^*$) and dielectric ($f > f^*$) regimes.

$= 6.12 \times 10^{-8} \Omega^{-1} \text{ m}^{-1}$, $\epsilon_{\parallel} = 4.08$, and $\epsilon_{\perp} = 4.50$, respectively. Here, the subscripts \parallel and \perp represent the orientations par-

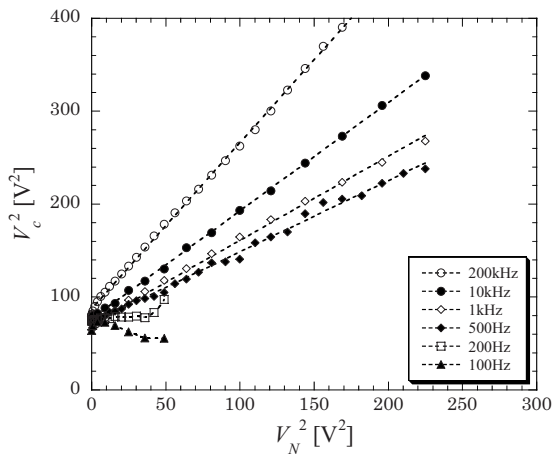


FIG. 3. Noise intensity (V_N) dependence of threshold (V_c) for WDs in the conduction regime (at a fixed ac frequency $f = 30$ Hz $< f^*$). By changing the cut-off frequency f_c of the noise, the theoretical linear relation ($V_c^2 = V_{c0}^2 + bV_N^2$) was investigated. Here, V_{c0} indicates the threshold ac voltage in the absence of noise ($V_N = 0$), and the slope b indicates the sensitivity of EHCs to noise. In the case of sufficiently colored noises (e.g., $f_c = 100, 200$ Hz $< f^*$), the relation is invalid (see text).

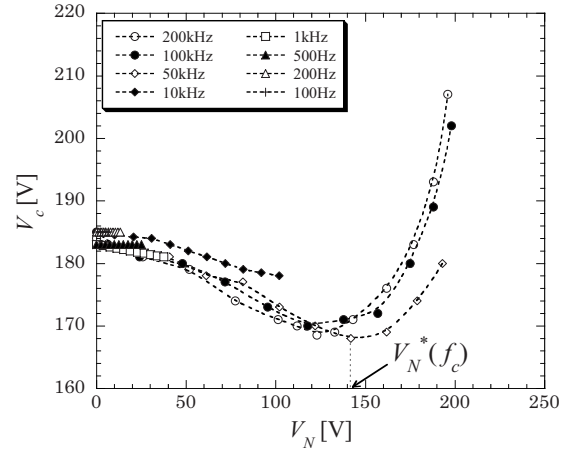


FIG. 4. Noise intensity (V_N) dependence of the threshold (V_c) for CVs in the dielectric regime (at a fixed ac frequency $f = 350$ Hz $> f^*$). By changing the cut-off frequency f_c of the noise, the variation in V_c was measured. In the case of the noises with $f_c = 100$ Hz ~ 10 kHz, V_c for higher V_N could not be measured owing to experimental limitations of the setup.

allel and perpendicular to the director of the NLC, respectively. The details of experimental setup are shown in our earlier report [33].

III. RESULTS AND DISCUSSIONS

A. EHCs in the absence of noise

Before dealing with the effects of noise on EHCs, we investigated the characteristics of thresholds and wavelengths in pattern formations *in the absence of noise*.

First, we measured thresholds V_c for the onset of the corresponding pattern formations in the conduction ($f < f^*$) and dielectric regimes ($f > f^*$) as shown in Fig. 2(a). The thresh-

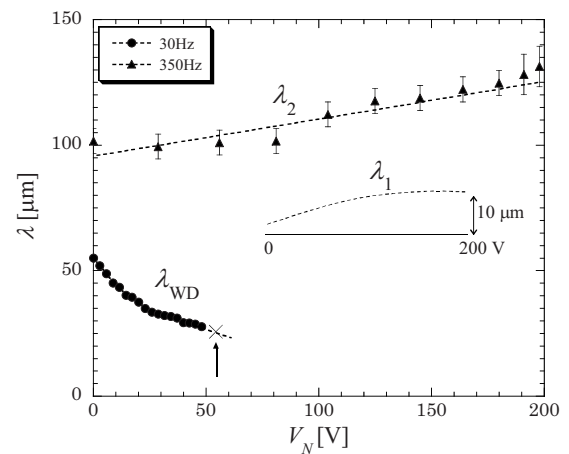


FIG. 5. Noise intensity (V_N) dependence of wavelengths [λ_{WD} , λ_1 , and λ_2 at their thresholds $V_c(V_N)$] in the conduction (at a fixed ac frequency $f = 30$ Hz $< f^*$) and the dielectric (at $f = 350$ Hz $> f^*$) regimes in the presence of white noise (with a fixed cutoff frequency $f_c = 500$ kHz $\gg f^*$). Here, λ_1 was estimated from Fig. 7. A localized wormlike pattern (WP) begins to appear around the point \times , as shown Fig. 6(c). See Figs. 6 and 7 for the corresponding pattern evolutions.

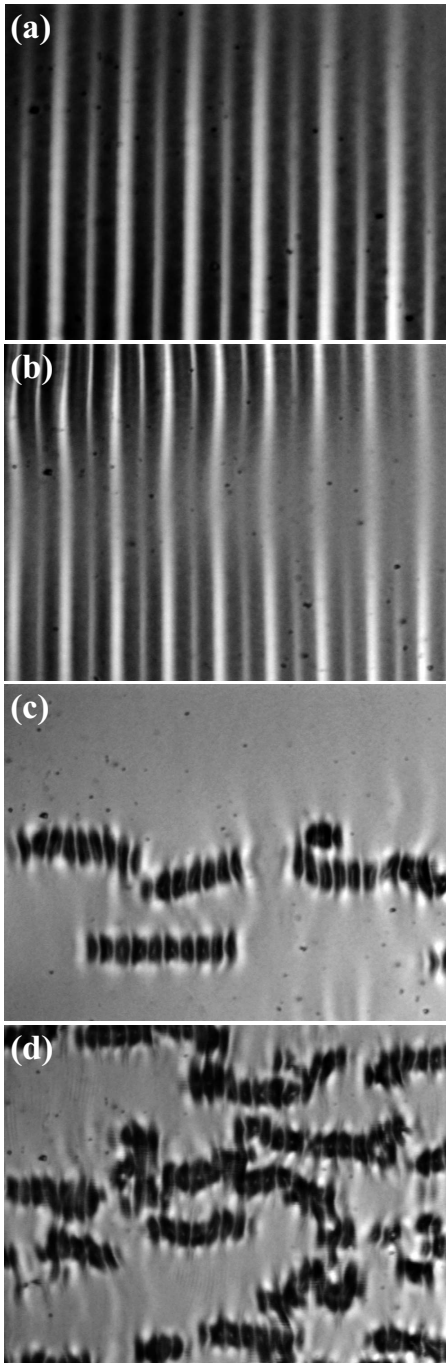


FIG. 6. Pattern evolutions in the conduction regime [at a fixed ac frequency $f=30 \text{ Hz} < f^*$ and $V_c(V_N)$] in the presence of white noise (with a fixed cut-off frequency $f_c=500 \text{ kHz} \gg f^*$). In order to obtain more visual patterns, each pattern was observed slightly above the threshold $V_c(V_N)$ for each $V_N=(a) 0$, (b) 18.2, (c) 54.0, (d) 65.1 V. A stationary WD evolves into a nonstationary WP with increasing V_N . See the corresponding variation in wavelength λ_{WD} shown in Fig. 5.

old curves show typical behavior for EHCs in the conduction [$V_c \sim (1+4\pi^2 f^2 \tau_\sigma^2)/[\xi^2 - (1+4\pi^2 f^2 \tau_\sigma^2)]$; ξ indicates the Helfrich parameter determined by combining some material constants of the NLC] and dielectric ($V_c \sim f^{1/2}$) regimes

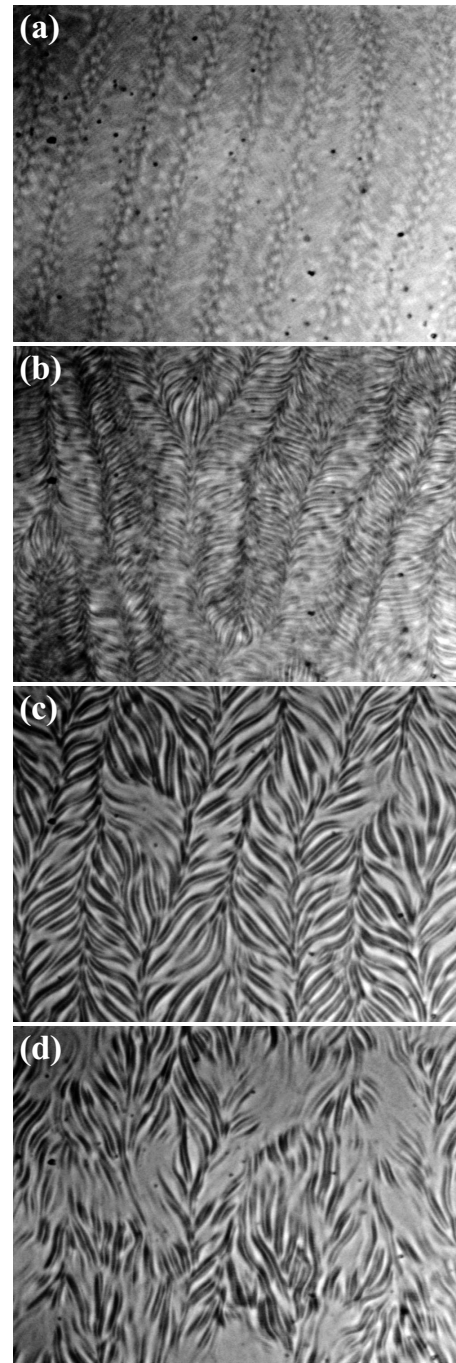


FIG. 7. Pattern evolutions in the dielectric regime [at a fixed ac frequency $f=350 \text{ Hz} > f^*$ and $V_c(V_N)$] in the presence of white noise (with a fixed cutoff frequency $f_c=500 \text{ kHz} \gg f^*$). In order to obtain more visual patterns, each pattern was observed slightly above the threshold $V_c(V_N)$ for each $V_N=(a) 0$, (b) 71.2, (c) 146, (d) 191 V. With increasing V_N , λ_1 increases remarkably, whereas λ_2 increases slightly. See the corresponding variation in wavelengths λ_1 and λ_2 shown in Fig. 5.

[2–6,12,13], for which a characteristic ac frequency f^* ($\sim 265 \text{ Hz}$) was determined.

Next, the characteristic wavelengths for both regimes were measured as a function of f at their thresholds. We defined λ_{WD} as the wavelength for a spatial periodicity (i.e.,

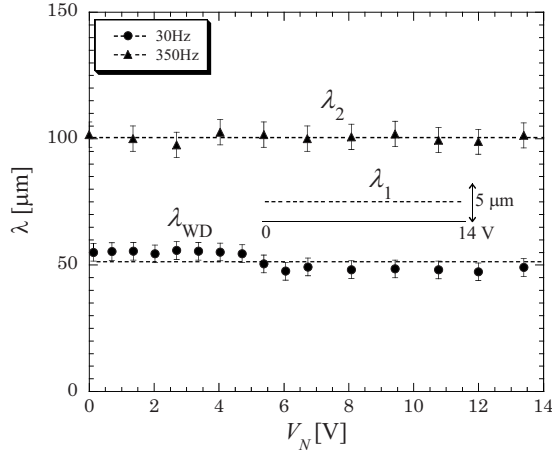


FIG. 8. Noise intensity (V_N) dependence of wavelengths [λ_{WD} , λ_1 , and λ_2 at their thresholds $V_c(V_N)$] in the conduction (at a fixed ac frequency $f=30$ Hz $< f^*$) and dielectric (at $f=350$ Hz $> f^*$) regimes in the presence of sufficiently colored noise (with a fixed cut-off frequency $f_c=200$ Hz $< f^*$). Here, λ_1 was estimated from optical observation. In this case, no variation in wavelengths λ_1 and λ_2 for CVs was found within experimental limitations [$V_N f_c = 500$ Hz] < 14 V] and error range, and λ_{WD} for WDs remains almost constant.

a pair of clockwise and counterclockwise vortices in WDs) as shown in Fig. 1(a). For CVs in the dielectric regime, on the other hand, we defined λ_1 as the short wavelength for the striated rolls, and λ_2 as the long wavelength for a pair of bands with alternating zig and zag rolls as shown in Fig. 1(b). As can be seen in Fig. 2(b), λ_{WD} (\sim order of d) decreases smoothly with increasing f , whereas λ_1 (~ 3.5 μm ; $\sim \lambda_2/30$) and λ_2 ($\sim 2d$) remain almost unchanged. In fact, CVs take place as a secondary instability slightly above the onset of convection V_c [12]. However, we measured λ_1 and λ_2 at V_{CV} for CVs because λ_2 ($\rightarrow \infty$) cannot be defined from the WD-like striated rolls (i.e., prechevron [12]) at V_c , and λ_1 remains unchanged between V_c and V_{CV} . Hereafter, λ_1 and λ_2 are regarded as the wavelengths of CVs at the onset of EHCs (i.e., $V_{CV} \rightarrow V_c$). Moreover, it is worth mentioning that the length $\lambda_2/2$ ($\sim d$) for CVs originates from the inertia (or prewavy) mode below V_c [12,14].

B. Effects of noise on onset of EHCs

We investigated threshold variations in pattern formations in the presence of noise. With varying cut-off frequency f_c of noise, we measured the noise intensity (V_N) dependence of the thresholds (V_c) for both regimes. Figure 3 shows the behavior of $V_c(V_N)$ for WDs in the conduction regime (at a fixed ac frequency $f=30$ Hz $< f^*$). The linear relation ($V_c^2 = V_{c0}^2 + bV_N^2$) common in previous theoretical and experimental studies [21,22,25–32] is confirmed again for higher f_c (500 Hz \sim 200 kHz $> f^*$). Noises with higher f_c ($> f^*$) play a role in the stabilization effect to the initial state. Accordingly, a shift in the ac threshold V_c is achieved by increasing the noise intensity (i.e., the slope $b > 0$ in Fig. 3). Moreover, the sensitivity of EHCs to noise (i.e., the slope b of the linear relation) weakens with decreasing f_c . However, the behavior

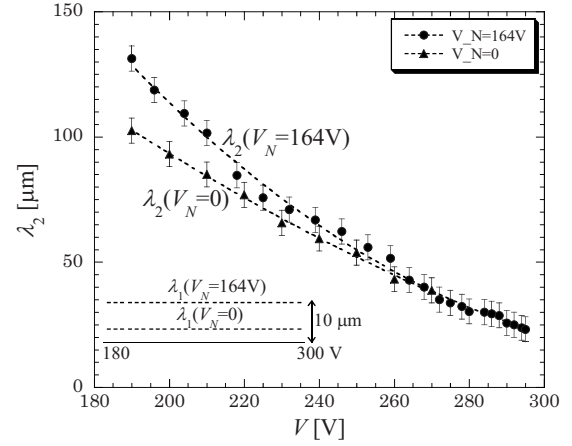


FIG. 9. Variation in wavelengths λ_1 and λ_2 for CVs with increasing ac voltage V (at a fixed frequency $f=350$ Hz $> f^*$) in the absence ($V_N=0$) and presence ($V_N=164$ V, $f_c=500$ kHz $\gg f^*$) of noise. Here, λ_1 appears to be unchanged with increasing V for both cases, whereas $\lambda_2(V)$ behaves similarly. See the corresponding pattern evolutions shown in Figs. 10 and 11.

of $V_c(V_N)$ for lower f_c (100, 200 Hz $< f^*$) deviates from this relation [28]. With respect to the intensity of noise, sufficiently colored noises (e.g., $f_c=100, 200$ Hz $< f^*$) exert not only a stabilization effect ($b > 0$) but also a destabilization effect ($b < 0$ in the case of $f_c=100$ Hz in Fig. 3) and no effect (neutral) leading to the onset of EHCs in some cases [e.g., $b=0$ ($0 < V_N < 6$ V) for $f_c=200$ Hz in Fig. 3]. Such changes in the effects depending on temporal characteristic of noise were also found in EHCs superposed with dichotomous noises [27,30].

On the other hand, Fig. 4 shows the behavior of $V_c(V_N)$ for CVs in the dielectric regime (at a fixed ac frequency $f=350$ Hz $> f^*$). Obviously, the effects of noise in this regime are markedly different from those in the conduction regime ($f=30$ Hz $< f^*$). For higher f_c of noise ($f_c \geq 50$ kHz), $V_c(V_N)$ has a minimal value at a certain characteristic intensity (V_N^*) of the noise (e.g., $V_c=168$ V at $V_N^*=140$ V and $f_c=50$ kHz). This means that the onset of EHCs can be induced at minimal electric force with the aid of an appropriate intensity of noise. This V_N -dependent behavior of V_c is reminiscent of stochastic resonance in spatially extended systems [35]. Although no measurement of $V_c(V_N)$ was carried out at large intensity V_N for lower f_c (1 \sim 10 kHz), owing to experimental limitations, it appears to behave similarly to the case of white noise with higher f_c (≥ 50 kHz). It can be said that in the case of the dielectric regime the intensity of noise has more remarkable effect on the threshold shift, independent of f and f_c ($\gg f^*$) [33]. However, in the case of sufficiently colored noises ($f_c=100$ –500 Hz), such behavior of $V_c(V_N)$ appears to disappear.

The basic argument regarding these effects of noise is as follows. By considering the underlying mechanisms of dissipative structures (WDs and CVs) in the corresponding regimes, the differing behavior of $V_c(V_N)$ between both regimes may be understood. As described in Sec. I, CVs are oscillating director structures in bulk, whereas WDs are large-scale convections over the whole bulk and require a

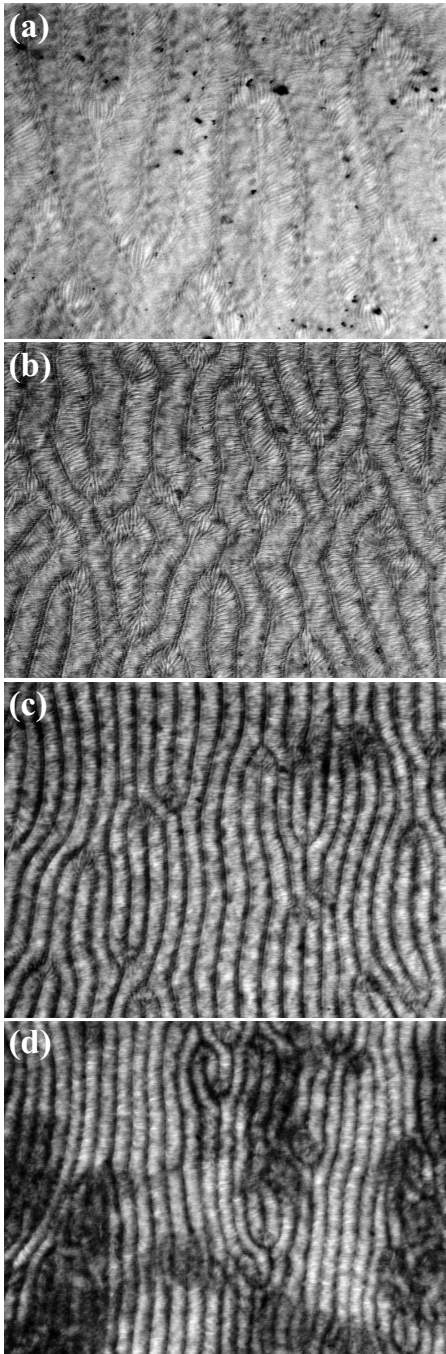


FIG. 10. Pattern evolutions with increasing ac voltage V (at a fixed frequency $f=350\text{ Hz} > f^*$) in the absence of noise ($V_N=0$). Each pattern was observed at $V=(a)$ 190, (b) 210, (c) 230, (d) 240 V. See the corresponding variation in wavelengths λ_1 and λ_2 shown in Fig. 9.

periodic space-charge distribution. Since noises give rise to the obstruction of periodic charge injections from electrodes and the random recombination of space charges, they suppress the instability of the periodic convection (WD). Thus, a higher deterministic field is needed to occur WDs in the presence of noise; the noise-induced stabilization effect for WDs is realized. On the other hand, since the director oscillation (for CVs) requires stationary charge distributions, a positive charge region in space should always be positive and a nega-

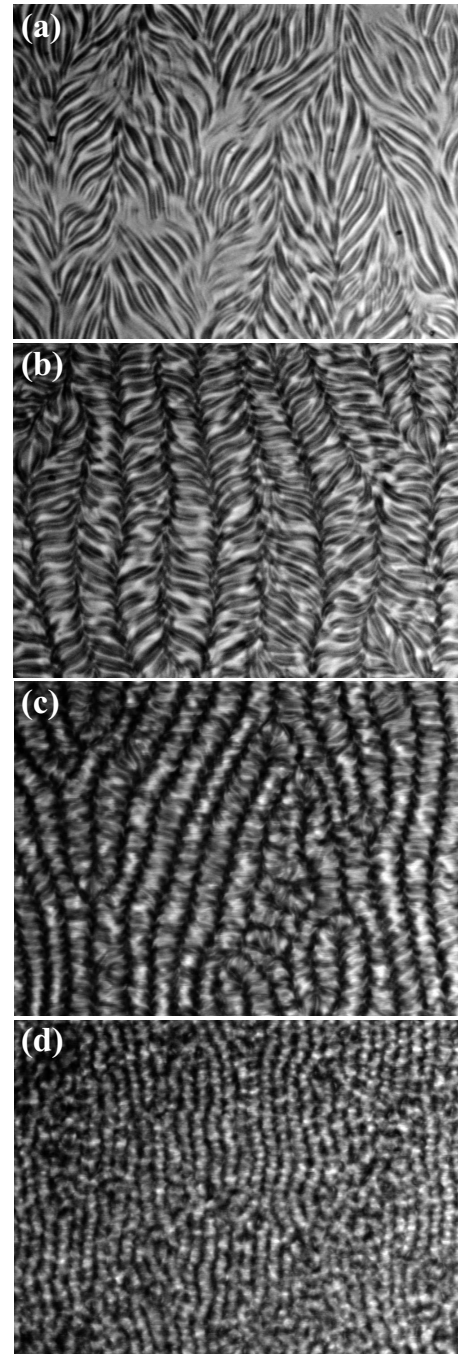


FIG. 11. Pattern evolutions with increasing ac voltage V (at a fixed frequency $f=350\text{ Hz} > f^*$) in the presence of white noise (with fixed $V_N=164\text{ V}$ and $f_c=500\text{ kHz} \gg f^*$). Each pattern was observed at $V=(a)$ 190, (b) 235, (c) 260, (d) 290 V. See the corresponding variation in wavelengths λ_1 and λ_2 shown in Fig. 9.

tive should be negative. For rather small-intensity noise, such charge distributions may hold with small modulations such as in some cases those of high amplitude and in some cases those of low amplitude, by a sufficiently high deterministic field superposed with the noise field. For superposition with high-intensity noise, however, noises certainly break the stationary space-charge distribution; that is, a positive charge region may change into negative and negative into positive. Nevertheless, in order to obtain the director

oscillation (CV), a stationary space-charge distribution must be reconstructed by increasing the deterministic voltage, which thus leads to an upward threshold shift. This therefore occurs almost the same intensity between deterministic and stochastic voltages, about 180 V, for example. Here, optimal noise intensity phenomena such as stochastic resonance can be observed. Actual situations are more complicated concerning f_c -dependent noise. For $f_c < f^*$ (determined by the intrinsic property of the NLC) in the conduction regime, therefore, the usual stabilization effects of noise ($b > 0$) are diminished. Then, a part of the noise, in the form of cooperative signals with the ac field, gives rise to unusual destabilization effects ($b < 0$). For V_N beyond $V_N^*(f_c)$ in the dielectric regime, on the other hand, the effects of noise may become complicated owing to the large dissipative energy of small-scale convections and unconsidered modes (such as inertia or prewavy modes [12,14]) as well as the director oscillation. The effects of noise can be changed by dominant instabilities in the system. Unfortunately, there is no theoretical explanation for the noticeable effects of noise in this dielectric regime.

C. Effects of noise on pattern structures

In the presence of noise, we measured the characteristic wavelengths for the corresponding patterns (WDs and CVs) at the onset of EHCs in the conduction and dielectric regimes.

First, Fig. 5 shows λ_{WD} for WDs, and λ_1 and λ_2 for CVs in the case of *white noises* ($f_c = 500$ kHz $\gg f^*$; $\tau_N = 7.37$ s). In the conduction regime [at $f = 30$ Hz $< f^*$ and $V_c(V_N)$], λ_{WD} decreases smoothly with increasing V_N . Around $V_N = 50$ V, WDs are replaced by wormlike patterns [WPs: spatially localized patterns in Fig. 6(c)] [36]. As shown in Fig. 6, the worms have lengths of $2-6\lambda_{\text{WD}}$ and are almost parallel to the director \mathbf{n}_0 . They move very actively, couples with one another, and are dilacerated. With increasing V_N , the number of worms increases, and worm-aggregated turbulence forms in the whole cell. This turbulence was found to be indistinguishable from the well-known dynamic scattering mode (DSM) [37]. Moreover, the transition from DSM1 to DSM2 [38] was observed. In the dielectric regime [at $f = 350$ Hz $> f^*$ and $V_c(V_N)$], on the other hand, λ_1 increases smoothly with increasing V_N and saturates at a certain value V_N as shown in Figs. 5 and 7. Here, λ_2 also increases slightly with increasing V_N . Similar to the conduction regime ($f < f^*$), CVs evolve into DSMs at larger V_N in the dielectric regime ($f > f^*$). However, wormlike localized patterns cannot be found in this dielectric regime because WPs originate from large-scale convections in bulk (in the conduction regime).

Next, Fig. 8 shows λ_{WD} for WDs, and λ_1 and λ_2 for CVs in the case of sufficiently *colored noises* ($f_c = 200$ Hz $< f^*$; $\tau_N = 403$ s). In contrast to the results for the white noises ($f_c \gg f^*$), λ_1 and λ_2 remain unchanged with increasing V_N (> 14 V in experimental limitations) in the dielectric regime [at $f = 350$ Hz and $V_c(V_N)$], and λ_{WD} remains almost constant within $V_N > 14$ V in the conduction regime [at $f = 30$ Hz and $V_c(V_N)$]. Therefore, it can be said that white noises ($f_c \gg f^*$) are more effective than colored noises ($f_c < f^*$) for controlling the pattern structures.

D. Pattern evolutions for chevrons with increasing ac voltage

Finally, we measured the variation in wavelengths λ_1 and λ_2 for CVs with increasing ac voltage V (at a fixed ac frequency $f = 350$ Hz and fixed noise intensity $V_N = 0$ and 164 V) in order to compare these with the above-described results in the case of increasing V_N . Figure 9 shows the similar behavior of λ_2 (V) in the absence ($V_N = 0$) and presence ($V_N = 164$ V and $f_c = 500$ kHz) of noise, which is also confirmed in actual images of pattern evolutions in Figs. 10 and 11. However, λ_1 seems to remain unchanged with increasing V as also shown in Figs. 10 and 11. The lengths of λ_1 ($V_N = 0$) and λ_1 ($V_N = 164$ V) are very different from each other [$\lambda_1(V_N = 0) < \lambda_1(V_N = 164$ V)]. Similar to the above-described results, moreover, CVs evolve into DSMs at larger V in both cases (i.e., fixed noise intensity $V_N = 0$ and 164 V). The important point is that the intensity V of the ac voltage varies λ_2 only, while λ_1 remains determined by the noise (with V_N and f_c) in both cases. On the other hand, the variation in wavelength λ_{WD} for WDs with increasing V was could not be measured because, with a small increase in V , WDs immediately evolved into fluctuating WDs and gridlike patterns [28].

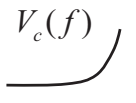
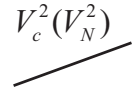
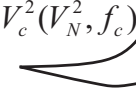

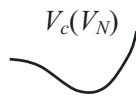
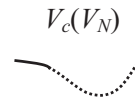
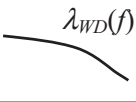
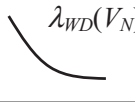
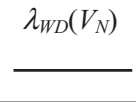


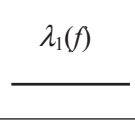
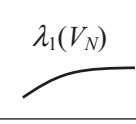
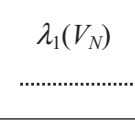

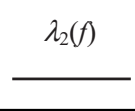
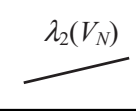
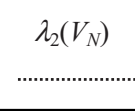
IV. SUMMARY

We investigated the effects of noise on the ac thresholds (V_c) for EHCs and the characteristic scales (wavelengths λ_{WD} for WDs and λ_1 and λ_2 for CVs) in the conduction and dielectric regimes. The experimental results for the threshold shifts and wavelengths in both regimes are summarized in Table I.

In the case of sufficiently colored noises ($f_c < f^*$), the dependence of the threshold [$V_c(V_N)$] on noise intensity is not the expected linear relation in the *conduction regime*. When sufficiently colored noises ($f_c < f^*$; e.g., $f_c = 100$ Hz in this study) are applied, the onset of convections could be induced below the threshold ac voltage V_{c0} determined in the absence of noise ($V_N = 0$). Such a noise-induced subthreshold instability is important for understanding nonlinear dissipative systems in noisy environments. In the *dielectric regime*, on the other hand, we found a peculiar dependence of threshold on noise intensity V_N , which has not been investigated in theoretical studies. This suggests that an optimal condition of noise with an appropriate intensity V_N and/or cut-off frequency f_c (or, τ_N) may aid the onset of convections so that EHCs occur at the lowest driving force. In other words, noise matching to an intrinsic time scale of the system facilitates instability (the oscillation of the director) most effectively, similar to stochastic resonance [15,16,35]. Such behavior of $V_c(V_N)$ may be explained by the difference in the pattern-formation mechanisms between both regimes.

The normal rolls (with wavelength λ_{WD}) for WDs showed different variation with respect to the intensity (V_N) and cut-off frequency (f_c) of the noise. On the other hand, the striated rolls (with λ_1) for CVs could be controlled by V_N and f_c although these were not varied with the intensity (V) and frequency (f) of the ac voltage. The ac voltage controls only the bands (with $\lambda_2/2$) for CVs, whereas the noise varies the λ_1 as well as the λ_2 of CVs. This means that λ_2 determined

TABLE I. Variation in the thresholds and wavelengths for EHCs with respect to the superposition of noise. Solid lines were directly measured and broken lines were estimated by optical observation.

		Conduction regime ($f < f^*$)			Dielectric regime ($f > f^*$)		
		without noise	white noise ($f_c > f^*$)	colored noise ($f_c < f^*$)	without noise	white noise ($f_c \gg f^*$)	colored noise ($f_c < f^*$)
Thresholds							
Wave-lengths	λ_{WD}						
	λ_1						
	λ_2						

by the inertia (or prewavy) mode may be controlled only by the intensity of the driving force (i.e., effective voltage) without regard to noise or ac voltage. Such effective voltage dependence was also found for the threshold problem of the Fredericks transition in NLCs [34]. Therefore, λ_1 is the most meaningful structure controlled only by white noises ($f_c \gg f^*$). In the case of sufficiently colored noises ($f_c < f^*$), however, no change in corresponding patterns (λ_{WD} , λ_1 , and λ_2) in the conduction and dielectric regimes was found with varying intensity of noise. These results show that dissipative structures as well as the onset of nonequilibrium systems can be controlled by noise with an appropriate timescale (f_c or

τ_N) and intensity (V_N). The present results of the wavelength variations are quite useful for fabricating modulated polymer surfaces by means of EHCs [39]. These effects of noise provide us with useful information with which to consider noise-controlled applications in fields such as nanotechnology [40] and neuroscience [41], in which noise is unavoidable.

ACKNOWLEDGMENTS

This study was partly supported by a Grant-in-Aid for Scientific Research from the Ministry of Education, Culture, Sports, Science and Technology of Japan and the Japan Society for the Promotion of Science (Grants No. 18540377, No. 20111003, and No. 21340110).

- [1] M. C. Cross and P. C. Hohenberg, *Rev. Mod. Phys.* **65**, 851 (1993).
- [2] L. Kramer and W. Pesch, *Annu. Rev. Fluid Mech.* **27**, 515 (1995).
- [3] Orsay Liquid Crystal Group, *Mol. Cryst. Liq. Cryst.* **12**, 251 (1971).
- [4] I. W. Smith, Y. Galerne, S. T. Lagerwall, E. Dubois-Violette, and G. Durand, *J. Phys. (Paris), Colloq.* **C1**, 237 (1975).
- [5] S. Kai and W. Zimmermann, *Suppl. Prog. Theor. Phys.* **99**, 458 (1989).
- [6] L. Kramer, A. Hertrich, and A. Pesch, in *Pattern Formation in Complex Dissipative Systems*, edited by S. Kai (World Scientific, Singapore, 1992), p. 238.
- [7] H. Richter, N. Klöpper, A. Hertrich, and A. Buka, *Europhys. Lett.* **30**, 37 (1995).
- [8] W. Pesch and U. Behn, in *Evolution of Spontaneous Structures in Dissipative Continuous Systems*, edited by F. H. Busse and S. C. Mueller (Springer, New York, 1998).
- [9] R. Williams, *J. Chem. Phys.* **39**, 384 (1963).
- [10] E. F. Carr, *Mol. Cryst. Liq. Cryst.* **7**, 253 (1969).
- [11] W. Helfrich, *J. Chem. Phys.* **51**, 4092 (1969).
- [12] L. M. Blinov, *Electro-optical and Magneto-optical Properties of Liquid Crystals* [The Universities Press (Belfast), Northern Ireland, 1983].
- [13] P. G. de Gennes and J. Prost, *The Physics of Liquid Crystals*, 2nd ed. (Oxford University Press, New York, 1993).

- [14] A. G. Rossberg and L. Kramer, *Physica D* **115**, 19 (1998); A. Buka, P. Toth, N. Eber, and L. Kramer, *Phys. Rep.* **337**, 157 (2000); J.-H. Huh, Y. Hidaka, A. G. Rossberg, and S. Kai, *Phys. Rev. E* **61**, 2769 (2000); H. Sakaguchi and A. Matsuda, *Physica D* **238**, 1 (2009).
- [15] R. Benzi, G. Parishi, A. Suter, and A. Vulpiani, *Tellus* **34**, 10 (1982).
- [16] L. Gammaitoni, P. Hänggi, P. Jung, and F. Marchesoni, *Rev. Mod. Phys.* **70**, 223 (1998); T. Mori and S. Kai, *Phys. Rev. Lett.* **88**, 218101 (2002).
- [17] W. Horsthemke and R. Lefever, *Noise-Induced Transitions* (Springer-Verlag, Berlin, 1984).
- [18] J. Garcia-Ojalvo and J. M. Sancho, *Noise in Spatially Extended Systems* (Springer-Verlag, New York, 1999).
- [19] R. Kawai, X. Sailer, L. Schimansky-Geier, and C. Van den Broeck, *Phys. Rev. E* **69**, 051104 (2004).
- [20] F. Sagués, J. M. Sancho, and J. García-Ojalvo, *Rev. Mod. Phys.* **79**, 829 (2007).
- [21] S. Kai, T. Kai, M. Takata, and K. Hirakawa, *J. Phys. Soc. Jpn.* **47**, 1379 (1979).
- [22] H. Brand and A. Schenzle, *J. Phys. Soc. Jpn.* **48**, 1382 (1980).
- [23] M. W. Evans, M. Ferrario, and P. Grigolini, *Physica A* **111**, 255 (1982).
- [24] N. Hashimoto, *J. Phys. Soc. Jpn.* **75**, 084002 (2006).
- [25] T. Kawakubo, A. Yanagita, and S. Kabashima, *J. Phys. Soc. Jpn.* **50**, 1451 (1981).
- [26] H. R. Brand, S. Kai, and S. Wakabayashi, *Phys. Rev. Lett.* **54**, 555 (1985).
- [27] U. Behn and R. Müller, *Phys. Lett.* **113A**, 85 (1985); R. Müller and U. Behn, *Z. Phys. B: Condens. Matter* **69**, 185 (1987).
- [28] S. Kai, H. Fukunaga, and H. Brand, *J. Phys. Soc. Jpn.* **56**, 3759 (1987); *J. Stat. Phys.* **54**, 1133 (1989).
- [29] S. Kai, M. Imasaki, S. Yamaguchi, and F. Sagues, in *Research of Pattern Formation*, edited by R. Takaki (KTK Scientific Publishers, Tokyo, 1994), p. 343.
- [30] U. Behn, A. Lange, and T. John, *Phys. Rev. E* **58**, 2047 (1998).
- [31] T. John, R. Stannarius, and U. Behn, *Phys. Rev. Lett.* **83**, 749 (1999); T. John, U. Behn, and R. Stannarius, *Phys. Rev. E* **65**, 046229 (2002).
- [32] J.-H. Huh, *J. Phys. Soc. Jpn.* **76**, 033001 (2007).
- [33] J.-H. Huh and S. Kai, *J. Phys. Soc. Jpn.* **77**, 083601 (2008).
- [34] J.-H. Huh and S. Kai, *J. Phys. Soc. Jpn.* **78**, 043601 (2009); **78**, 083601 (2009).
- [35] H. S. Wio, *Phys. Rev. E* **54**, R3075 (1996); H. S. Wio, S. Bouzat, and B. von Haefen, *Physica A* **306**, 140 (2002); H. L. Wang, K. Zhang, and Q. Ouyang, *Phys. Rev. E* **74**, 036210 (2006).
- [36] M. Dennin, G. Ahlers, and D. S. Cannell, *Phys. Rev. Lett.* **77**, 2475 (1996); H. Riecke and G. D. Granzow, *ibid.* **81**, 333 (1998); U. Bisang and G. Ahlers, *Phys. Rev. E* **60**, 3910 (1999).
- [37] C. Deutsch and P. N. Keating, *J. Appl. Phys.* **40**, 4049 (1969).
- [38] S. Kai, W. Zimmermann, M. Andoh, and N. Chizumi, *Phys. Rev. Lett.* **64**, 1111 (1990).
- [39] A. Hoischen, S. A. Benning, and H.-S. Kitzrowa, *J. Appl. Phys.* **105**, 013540 (2009).
- [40] G. Stegemann, A. G. Balanov, and E. Schöll, *Phys. Rev. E* **71**, 016221 (2005).
- [41] G. M. Süel, J. Garcia-Ojalvo, L. M. Liberman, and M. B. Elowitz, *Nature (London)* **440**, 545 (2006); N. Rosenfeld, J. W. Young, U. Alon, P. S. Swain, and M. B. Elowitz, *Science* **307**, 1962 (2005).